

Sequential Hydration Energies of the Sulfate Ion, from Determinations of the Equilibrium Constants for the Gas-Phase Reactions: $\text{SO}_4(\text{H}_2\text{O})_n^{2-} = \text{SO}_4(\text{H}_2\text{O})_{n-1}^{2-} + \text{H}_2\text{O}$

Arthur T. Blades and Paul Kebarle*

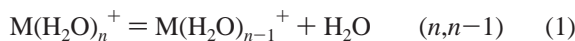
Department of Chemistry, University of Alberta, Edmonton, Alberta, Canada T6G 2G2

Received: July 21, 2005

Sequential hydration energies of $\text{SO}_4(\text{H}_2\text{O})_n^{2-}$ were obtained from determinations of the equilibrium constants of the following reactions: $\text{SO}_4(\text{H}_2\text{O})_n^{2-} = \text{SO}_4(\text{H}_2\text{O})_{n-1}^{2-} + \text{H}_2\text{O}$. The SO_4^{2-} ions were produced by electrospray and the equilibrium constants $K_{n,n-1}$ were determined with a reaction chamber attached to a mass spectrometer. Determinations of $K_{n,n-1}$ at different temperatures were used to obtain $\Delta G_{n,n-1}^0$, $\Delta H_{n,n-1}^0$, and $\Delta S_{n,n-1}^0$ for $n = 7$ to 19. Interference of the charge separation reaction $\text{SO}_4(\text{H}_2\text{O})_n^{2-} = \text{HSO}_4(\text{H}_2\text{O})_{n-k}^- + \text{OH}(\text{H}_2\text{O})_{k-1}^-$ at higher temperatures prevented determinations for $n < 7$. The $\Delta S_{n,n-1}^0$ values obtained are unusually low and this indicates very loose, disordered structures for the $n \geq 7$ hydrates. The $\Delta H_{n,n-1}^0$ values are compared with theoretical values $\Delta E_{n,n-1}$, obtained by Wang, Nicholas, and Wang. Rate constant determinations of the dissociation reactions $n, n-1$, obtained with the BIRD method by Wong and Williams, showed relatively lower rates for $n = 6$ and 12, which indicate that these hydrates are more stable. No discontinuities of the $\Delta G_{n,n-1}^0$ values indicating an unusually stable $n = 12$ hydrate were observed in the present work. Rate constants evaluated from the $\Delta G_{n,n-1}^0$ results also fail to indicate a lower rate for $n = 12$. An analysis of the conditions used in the two types of experiments indicates that the different results reflect the different energy distributions expected at the dissociation threshold. Higher internal energies prevail in the equilibrium measurements and allow the participation of more disordered transition states in the reaction.

1. Introduction

Determinations involving singly charged positive or negative ions and solvent molecules, such as H_2O

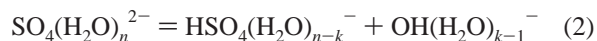


or other ligands, that lead to sequential enthalpies $\Delta H_{n,n-1}^0$ and entropies $\Delta S_{n,n-1}^0$ with a high-pressure mass spectrometer, were initiated some 40 years ago.¹ These determinations have provided a wealth of data on ion–solvent and ion–ligand interactions.² The development of theoretical calculations³ and experimental studies involving ion–molecule clusters produced in molecular beams⁴ were also stimulated. The quoted work^{1–4} gives only representative samples of early work from a very large number of publications in each area.

The early studies of ion equilibria were limited to singly charged ions yet multiply charged ions such as Mg^{2+} , Ca^{2+} , Fe^{2+} , Zn^{2+} , SO_4^{2-} , HPO_4^{2-} , etc. are of paramount importance in condensed-phase chemistry and biochemistry. However, these ions were very difficult to produce in the gas phase. The electrospray ionization method (ESI), developed in the nineteen eighties,⁵ with which ions present in a solution can be transferred to the gas phase, was used⁶ to solve this problem and led to the first systematic studies of multiply charged ion–ligand complexes.⁶

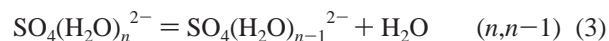
The first experimental studies of the SO_4^{2-} hydrates in the gas phase⁷ were restricted to collision-induced dissociation (CID) experiments. It was found that the high n hydrates,

$\text{SO}_4(\text{H}_2\text{O})_n^{2-}$, lose H_2O when exposed to CID, while the low n hydrates ($n < 4$) undergo preferentially charge separation:



The experiments⁷ also showed that the completely dehydrated SO_4^{2-} is unstable in the gas phase—it undergoes electron detachment. A prediction that SO_4^{2-} is unstable and undergoes electron detachment based on theoretical calculations was made at about the same time.⁸

Hydration equilibrium determinations⁹ at room temperature were performed later. $\text{SO}_4(\text{H}_2\text{O})_n^{2-}$ ions obtained at atmospheric pressure with ESI of solutions of sodium or potassium sulfate were introduced into a reaction chamber at room temperature that contained N_2 bath gas at 10 Torr and known partial pressures of H_2O . The present work is based on determinations with a redesigned¹⁰ reaction chamber that can operate at different temperatures. This allows determination not only of the free energy change at a single temperature, but also via van't Hoff plots of the enthalpy and entropy changes (eqs 3–5).



$$\Delta G_{n,n-1}^0 = -RT \ln K_{n,n-1} \quad (4)$$

$$\Delta G_{n,n-1}^0 = \Delta H_{n,n-1}^0 - T\Delta S_{n,n-1}^0 \quad (\text{at constant } T) \quad (5)$$

Determinations of the equilibria (eq 3) became difficult at low n , which require higher temperatures, because of interference of charge separation reactions that lead to hydrated HSO_4^- and hydrated OH^- (eq 2). The interference occurs even when

* Address correspondence to this author. E-mail: paul.kebarle@ualberta.ca.

the charge separation reaction is considerably slower than the forward and reverse reactions of the equilibrium (eq 3). This happens because the charge separation is a totally irreversible reaction due to the Coulombic repulsion of the HSO_4^- and OH^- ions (for some details on charge separation reactions, see ref 11 and references therein). Due to reaction 2, the concentration of the hydrated sulfate ions at equilibrium decreases continuously during the full residence time of the ions in the reaction chamber. Because of this difficulty, reliable values could not be obtained for $n < 7$.

While thermodynamic values for low n would have been useful, they are not absolutely essential because modern theoretical calculations of the energies of SO_4^{2-} and of the low n hydrates are available.¹² Furthermore, theoretical calculation of the thermodynamic values ΔH_n^0 and ΔS_n^0 based on theoretically evaluated vibrational frequencies and rotational moments of inertia can be routinely performed. At low n , such theoretical predictions would be of accuracy similar to the experimental data based on ion equilibria. However, at high n where the bonding of the water molecules becomes weak, the theoretical evaluations of the third law entropies based on separate vibrational, rotational, and translational motions can become questionable particularly when the harmonic oscillator approximation is used. Therefore, experimental results at high n are particularly important. As will be seen, the present experimental results for $\Delta S_{n,n-1}^0$ of the high n hydrates indicate the presence of very free motions of the H_2O molecules within the water cluster that would not have been predicted with the ab initio calculations.

The $\Delta G_{n,n-1}^0$ for the dehydration reaction (eq 3) determined at a given temperature, T , provide a scale of the thermodynamic stabilities of the clusters with different n . Determinations of the relative stabilities of $\text{SO}_4(\text{H}_2\text{O})_n^{2-}$ have been obtained by Wang and co-workers,¹² who used theoretical calculations to determine the electronic dissociation energies $\Delta E_{n,n-1}$. Wang's results, which extend from $n = 1$ to 6, have some relevance for the present work which covers $n = 7$ to 19.

More recently, Wong and Williams¹³ have determined experimentally the kinetic rate constants for the dissociation of $\text{SO}_4(\text{H}_2\text{O})_n^{2-}$, with the BIRD technique in a Fourier transform ion cyclotron (FT-ICR) mass spectrometer. The energy for the dissociation of the ions in the vacuum of the mass spectrometer is provided by blackbody infrared radiation. These authors show that the reactions proceed by loss of a single H_2O molecule. Rate constants for the dissociation k_n were determined that cover the range of hydrates $n = 6$ to 17. Thus these results are even more relevant to the present work. The BIRD studies indicate that the $n = 6$ and 12 structures have special stability, i.e., are "magic" ions. The results^{12,13} are compared with the thermodynamic values obtained in the present work in the Results and Discussion section. The relative significance of magic ions in the BIRD experiments¹³ and the present thermochemical measurements is also considered.

2. Experimental Section

The apparatus used has been described in detail.¹⁰ Briefly, 1 $\mu\text{L}/\text{min}$ of a 1 mM solution of Na_2SO_4 in perdeuterated methanol is injected with a motor driven syringe into the electrospray capillary, which is at -3000 V. The capillary emits a plume of very small droplets into the atmospheric air. The droplets are charged by an excess of negative ions. Evaporation of the droplets in the plume of the spray leads to gas-phase negative ions. The plume of droplets and ions impinges on a stainless steel sampling capillary (-25 V) that leads to a fore chamber.

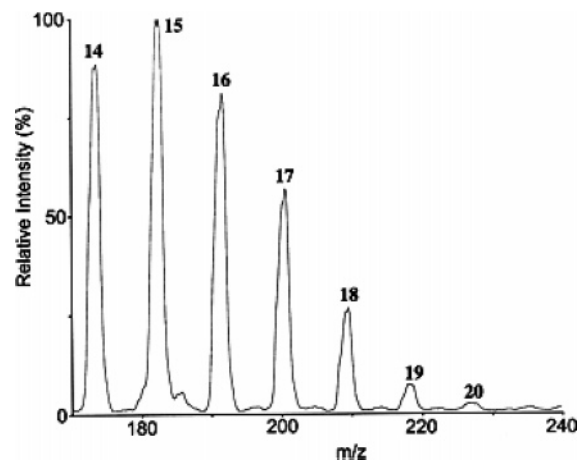


Figure 1. Partial mass spectrum of ions from the reaction chamber that shows ions with higher mass to charge (m/z) values. All major ions are due to $\text{SO}_4(\text{H}_2\text{O})_n^{2-}$ species. The value of n is given over each peak. The temperature was -18.6 °C. The partial pressure of water vapor in the reaction chamber was 140 mTorr. All the observed $\text{SO}_4(\text{H}_2\text{O})_n^{2-}$ ions are in hydration equilibrium.

A countercurrent of nitrogen gas around the entrance of the sampling capillary inhibits the entrance of methanol vapor in the sampling capillary while the ions guided by the potential drop enter the capillary. A weak electric field is used to drift the ions from the fore chamber to the reaction chamber. Both chambers are supplied with nitrogen gas at 10 Torr containing known partial pressures of the reagent gas H_2O in the 1–100 mTorr range. A very weak electric field drifts the ions through the reaction chamber. At the end of the chamber, some of the gas and ions effuse through a small orifice into the vacuum of the mass spectrometer. The residence time of the ions in the reaction chamber is estimated to be in the submillisecond range. Both fore and reaction chambers are maintained at the same temperature. The hydration equilibria establish in the reaction chamber. The ratio of the ion intensities detected with the mass spectrometer is assumed to be equal to the concentration ratio of the ions at the end of the reaction chamber:

$$I_n/I_{n-1} = [\text{SO}_4(\text{H}_2\text{O})_n^{2-}]/[\text{SO}_4(\text{H}_2\text{O})_{n-1}^{2-}] \quad (6)$$

When methanol is used as solvent with electrospray, a reaction occurs that leads to $\text{CH}_3\text{OCO}_2^-$ ions in the gas phase. To avoid interference of the monohydrate of this ion with the $n = 7$ hydrate of SO_4^- , perdeuterated methanol was used.

3. Results and Discussion

(a) **Experimental Determinations of $\Delta G_{n,n-1}^0$, $\Delta H_{n,n-1}^0$, and $\Delta S_{n,n-1}^0$.** Typical mass spectra observed on sampling the reaction chamber are shown in Figures 1 and 2. The conditions used lead to observed hydrated ions that are in equilibrium. The spectrum (Figure 1) was obtained at a relatively high partial pressure, $p(\text{H}_2\text{O}) = 140$ mTorr, and also a relatively low reaction chamber temperature of -18.6 °C. These conditions lead to formation of $\text{SO}_4(\text{H}_2\text{O})_n^{2-}$ hydrates with high n . The spectrum (Figure 2) was obtained at a higher temperature, of 9.5 °C, and lower pressure, $p(\text{H}_2\text{O}) = 4.7$ mTorr, and illustrates the formation of $\text{SO}_4(\text{H}_2\text{O})_n^{2-}$ hydrates with low n . Under these conditions one observes also the formation of HSO_4^- and its first hydrate $\text{HSO}_4(\text{H}_2\text{O})^-$. These singly charged ions are due to the charge separation reaction eq 2 discussed in the Introduction. The charge separation is fostered by low n $\text{SO}_4(\text{H}_2\text{O})_n^{2-}$ hydrates and high temperature. The much lower hydration of

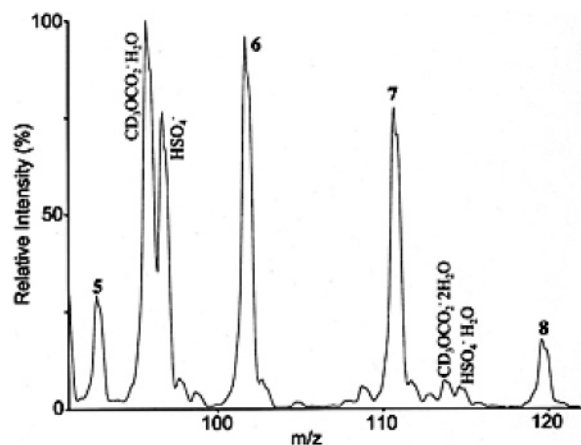


Figure 2. Major ions observed at higher, 9.5 °C, temperature and lower water vapor pressure, 4.7 mTorr, than used in Figure 1. These conditions foster the formation of low n , $\text{SO}_4(\text{H}_2\text{O})_n^{2-}$ hydrates at equilibrium, and also the irreversible charge separation: reaction $\text{SO}_4(\text{H}_2\text{O})_n^{2-} = \text{HSO}_4(\text{H}_2\text{O})_{n-k}^- + \text{OH}(\text{H}_2\text{O})_{k-1}^-$. In this mass range also the extraneous $\text{CD}_3\text{OCO}_2(\text{H}_2\text{O})_n^-$ with $n = 1$ and 2, is present. For its origin see the Experimental Section.

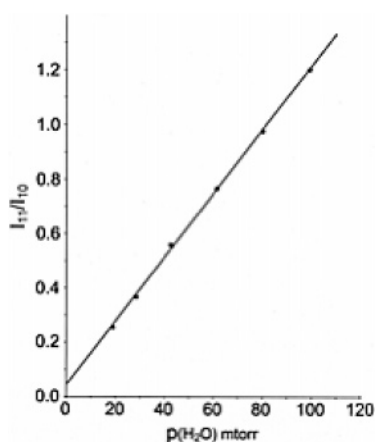
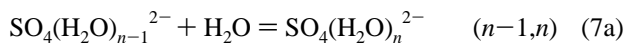


Figure 3. The intensity ratio of $\text{SO}_4(\text{H}_2\text{O})_n^{2-}$ ions with $n = 11$ and 10, obtained from six mass spectra with six different partial pressures of water and at a constant temperature of 21 °C, is plotted versus the corresponding water pressures. The straight line obtained obeys the equilibrium requirement, see eq 7. The ratio I_{11}/I_{10} divided by the water pressure equals the equilibrium constant $K_{10,11} = 11 \text{ Torr}^{-1}$ or $3.4 \times 10^{-16} (\text{molecules}/\text{cm}^3)^{-1}$.

the singly charged HSO_4^- relative to the SO_4^{2-} observed in Figure 2 illustrates the much higher hydrating power of the double charge.

An example of the experimental data used to determine the equilibrium constants is shown in Figure 3. It is based on the ion intensities I_n and I_{n-1} of the hydrates $n - 1 = 10$ and $n = 11$, determined from mass spectra obtained at six different water pressures and at a constant temperature of 21 °C. For ions that are at equilibrium, eq 7b should hold,



$$K_{n-1, n} = (I_n/I_{n-1})/p(\text{H}_2\text{O}) \quad (7b)$$

The plot of I_{11}/I_{10} versus $p(\text{H}_2\text{O})$ does lead to a straight line as required by eq 7b. However, there is a very small positive intercept of I_{11}/I_{10} at $p(\text{H}_2\text{O}) = 0$ that is not expected. Such small intercepts were found also in previous work. It was shown that the intercept is due to traces of water that are present in the N_2 bath gas used. Therefore, $K_{n-1, n}$ is evaluated with the

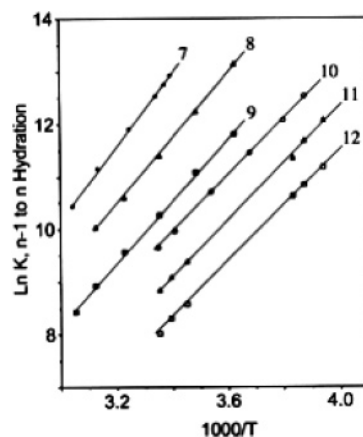


Figure 4. van't Hoff plots of the equilibrium constants $K_{n-1, n}$. The $K_{n-1, n}$ values used are from plots as in Figure 3, obtained at different temperatures. The values of n are given for each plot. The slopes of the straight line plots give the corresponding $-\Delta H_{n-1, n}^0$ values.

TABLE 1: Thermochemical Data for $n, n-1$ Reactions^{a, b}

n	ΔH^0	ΔS^0	ΔG^0 (298 K) ^c	ΔG^0 (270 K)
7	13.9	21.6	7.5 (7.5)	8.1
8	12.4	19.0	6.8 (6.7)	7.4
9	11.8	19.0	6.1 (6.0)	6.6
10	10.9	17.2	5.8 (5.5)	6.2
11	10.9	19.0	5.3	5.8
12	10.7	19.9	4.8	5.4
13				5.1
14				4.9
15				4.5
16				4.3
17				4.2
18				3.9
19				3.7

^a For the method used to obtain data see the Results and Discussion, Section a. ^b Values are for the $n, n-1$ reaction. ΔH^0 and ΔG^0 values are in kcal/mol, ΔS values are in cal/(deg mol). All values are for the reaction in the standard state of 1 atm. ^c ΔG^0 values in parentheses are results obtained in previous work, see Table 3 in Blades et al.⁹

slope of the (I_n/I_{n-1}) versus $p(\text{H}_2\text{O})$ plots. All the equilibrium constants used in the van't Hoff plots shown in Figure 4 were obtained from such plots, using several different water pressures.

The van't Hoff plots, $\ln K_{n-1, n}$ versus $1/T$, lead to a constant slope that equals $-\Delta H_{n-1, n}^0$ and is essentially independent of temperature in the temperature range used. Therefore, the corresponding $\Delta S_{n-1, n}^0$ values will be also essentially independent of the temperature. The $\Delta S_{n-1, n}^0$ values are obtained from $\Delta H_{n-1, n}^0$ and the available $\Delta G_{n-1, n}^0$ values are from $\Delta G_{n-1, n}^0 = RT \ln K_{n-1, n} = \Delta H^0 - T\Delta S^0$ (at constant T). The $\Delta G_{n-1, n}^0$, $\Delta H_{n-1, n}^0$, and $\Delta S_{n-1, n}^0$ values obtained are summarized in Table 1. The data given are not for the $n-1, n$ reaction but for the $n, n-1$ reaction, obtained with the relationship $\Delta G_{n-1, n}^0 = -\Delta G_{n, n-1}^0$, which holds also for ΔH^0 and ΔS^0 . The numerical data for the $n, n-1$ quantities are positive and more convenient for the following discussion.

(b) Discussion of Thermochemical Data, Table 1, and Comparison with Theoretical Results of Wang et al.¹² The $\Delta H_{7,6}^0$ is the enthalpy with lowest n in Table 1. As mentioned in the Introduction, measurements at lower n required higher temperature and this led to rapid disappearance of the $\text{SO}_4(\text{H}_2\text{O})_n^{2-}$ reactants with $n < 5$ by the charge separation reaction eq 2. Because these were in equilibrium with the higher n hydrates all SO_4^{2-} hydrates tended to be lost particularly at the lower water pressures.

Therefore, a direct comparison with the theoretical values $\Delta E_{n,n-1}$ of Wang et al.,¹² for values of $n = 1$ to 6, is not possible. Still, interesting insights are provided from an examination of the trends in the two sets of data. The theoretical results¹² were obtained with careful calculations based of density functional theory at the B3LYT/TZVP+ level, for details, see footnote 23 in Wang.¹² However, the vibrational frequencies were not evaluated. Therefore only the electronic energies without zero point vibrational energy correction are available. The values¹² (in kcal/mol) for the given $(n,n-1)$ are

$$\Delta E_{n,n-1} = 27.7 (1,0); 26.4 (2,1); 24.9 (3,2); \\ 23.5 (4,3); 22.4 (5,4); 21.8 (6,5) \text{ kcal/mol} \quad (8)$$

The most stable structures for $n = 1$ to 4 involve each water molecule interacting with two O atoms of the SO_4^{2-} . For $n = 5$ and 6, as the space near the sulfate oxygen becomes crowded, the two H bond interactions per water molecule are gradually replaced by H_2O molecules forming one H bond with a sulfate oxygen and another with an O of a neighboring water molecule, see structures in Figure 3,

Wong and Williams¹³ provide structures for $n = 4-13$, based on molecular modeling with the MMFF force field. These approximate predictions agree with the Wang et al.¹² geometries for $n = 4$ and 5. For $n = 6$, MMFF predicts a more compact structure where each water molecule forms two H bonds with sulfate oxygen, so that each sulfate oxygen interacts with three H atoms provided by three water molecules. For $n = 7$ to 12 the structures are looser and some of the water molecules move to "outer shell" positions where they bond only to other water molecules.

Making an extrapolation of the $\Delta E_{n,n-1}$ (eq 8) leads to an approximate range of $\Delta E_{7,6} = 21-19$ kcal/mol. A simple extrapolation would have led to a value of ~ 21 kcal/mol. The lower value of 19 kcal/mol takes into account that $n = 6$ may be a magic ion. In that case a larger drop would be expected. The experimental $\Delta H_{7,6}^0 = 13.9$ kcal/mol (Table 1) is still some 4 kcal/mol lower than the lower limit. While some differences between $\Delta E_{n,n-1}$ electronic and $\Delta H_{n,n-1}^0$ thermal are expected, the observed difference seems too large on the basis of similar comparisons in previous work.¹⁴ It is not clear whether the difference can be attributed entirely to errors in the calculation or experiment.

(c) Significance of $\Delta S_{n,n-1}^0$ and $\Delta G_{n,n-1}^0$ Results for Determinations of the Relative Stabilities of the $\text{SO}_4(\text{H}_2\text{O})_n^{2-}$ Hydrates and Magic Numbers for Hydrates of Unusual Stability. The observed entropy changes $\Delta S_{n,n-1}^0$ (Table 1) are in the 21–17 cal/(deg·mol) range. These values are low when compared with values observed for low n hydrates and strongly bonding ligands of the metal ions, Mg^{2+} , Ca^{2+} , and Zn^{2+} , which are in the range of 22–30 cal/(deg·mol) (see values in Table 1 in Peschke et al.^{14b}). On the other hand, for high n , the values^{14b} fall in the $\Delta S_{n,n-1}^0 = 19-22$ cal/(mol·deg) range.¹⁴ These low entropies were rationalized¹⁴ by the assumption that these outer shell water molecules are not only weakly bonded but also can move to other vacant positions. This can lead to a quasifree translation when a loose weakly bonded outer shell is present. The additional freedom provided leads to the low $\Delta S_{n,n-1}^0$ values observed.

The quasitranslational freedom is expected to be more pronounced for the $n > 6$ water molecules in the SO_4^{2-} system. Due to the large separation of the sulfate oxygen atoms, the negative charge is much more dispersed than is the case for the positive charge in the Mg^{2+} , Ca^{2+} , and Zn^{2+} ions. Therefore the bonding of the inner shell and outer shell molecules is

weaker. Furthermore, the presence of four sulfate oxygens provides a scaffold that could be facilitating the formation of multiple isomeric loose structures in the outer shell. This view is supported by the loose structures predicted by MMFF¹³ which indicate several isomeric structures for the same n . Transitions from one structure to the other may be facile and lead to a quasitranslation of the water molecules.

Wong and Williams¹³ also have reported determinations of the rate constants k_n for the dissociation of $\text{SO}_4(\text{H}_2\text{O})_n^{2-}$ hydrates with n in the range 6 to 17. The rate constants were determined with the BIRD technique in a Fourier transform ion cyclotron (FT-ICR) mass spectrometer. With BIRD, the energy for the dissociation of the ions in the vacuum of the ion cell is provided by the blackbody infrared radiation emitted from the cell walls. The experiments were performed with the ion cell walls at 21 °C. The authors showed that the reactions proceed by loss of a single H_2O molecule, i.e., the k_n rate constants determined¹³ from the dissociation rate of $\text{SO}_4(\text{H}_2\text{O})_n^{2-}$ correspond to the $k_{n,n-1}$ rate constants.

A correlation of the values of the rate constants, $k_{n,n-1}$, with the equilibrium constants, $K_{n-1,n}$, determined in the present work can be expected:

$$K_{n-1,n}^C = k_{n-1,n}/k_{n,n-1} \quad \text{or} \quad k_{n,n-1} = k_{n-1,n}/K_{n-1,n}^C \quad (9)$$

$K_{n-1,n}^C$ is the equilibrium constant where the reactants are in units of concentration rather than partial pressures as is the case for $K_{n-1,n}$. The equilibrium constant $K_{n-1,n}^C$ can be evaluated from $K_{n-1,n}$. Ion–molecule association reactions, including ion hydration reactions, proceed without activation energies¹⁵ and their rate constants can be predicted with the Langevin and ADO theory.¹⁵ The rate constants k are only weakly dependent on the properties of the ion and molecule and are found¹⁵ to be close to the value $k = 10^{-9} \text{ s}^{-1} \cdot (\text{molecules}/\text{cm}^3)^{-1}$. Using this value for all $k_{n-1,n}$ rate constants, one can obtain with eq 9 the corresponding $k_{n,n-1}$ values and compare those with the results obtained with BIRD. For example, the $K_{10,11}^C = 3.7 \times 10^{-16}$ (for concentration units in $\text{molecules}/\text{cm}^3$)⁻¹ at 21 °C, evaluated from the data in Figure 3, leads to $k_{11,10} = 2.7 \times 10^6 \text{ s}^{-1}$. The order of magnitude of this value is supported by the present experimental conditions which require $k_{n,n-1}$ values of the same order of magnitude.¹⁷ The $k_{11,10} = 2.7 \times 10^6 \text{ s}^{-1}$ value is 6 orders of magnitude larger than the value ($k_{11,10} = 2.4 \text{ s}^{-1}$) obtained at the same temperature with BIRD.

The temperature leading to the observed¹³ rate of 2.4 s^{-1} , when true Boltzmann conditions are present, can be evaluated with eq 9 and the $\Delta H_{11,10}^0$ and $\Delta S_{11,10}^0$ in Table 1. The result is ca. -108 °C.

The $k_{n,n-1}$ values for $n = 6$ to 19 obtained with BIRD¹³ and the present results, based on eq 9 and $K_{n-1,n}$ (obtained from the $\Delta G_{n,n-1}^0$ values at 270 K, Table 1), are shown in Figure 5. To accommodate the large spread of the $k_{n,n-1}$ values, a logarithmic scale is used. The $k_{n,n-1}$ based in Table 1 exhibit a large increase with n compared to the BIRD rate constants $k_{n,n-1}$ which show a minimal increase.

A linear plot of the rate constants versus n , see Figure 4, in Wong and Williams,¹³ indicated that the $k_{n,n-1}$ values for $n = 6$ and 12 exhibit downward deviations. These deviations are also discernible in the logarithmic plot (Figure 5). Low values for $k_{n,n-1}$ indicate more stable (magic) $\text{SO}_4(\text{H}_2\text{O})_n^{2-}$ hydrates. The theoretical DFT calculations by Wang et al.,¹² which extend up to $n = 6$, do support a more stable structure for the $n = 6$ hydrate. The molecular dynamics calculations of Wong and Williams which extend also to higher n do also support a more stable structure for $n = 6$ and at a stretch, also for $n = 12$.

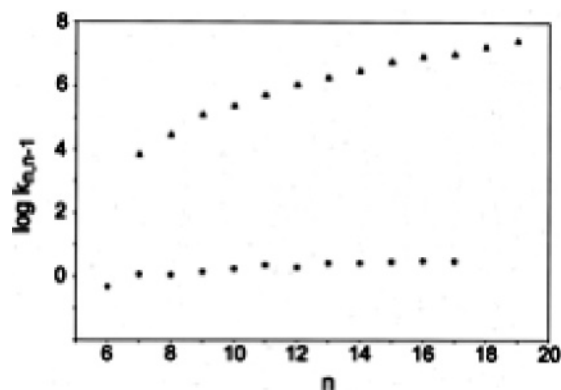


Figure 5. Comparison of rate constants $k_{n,n-1}$ obtained with BIRD¹³ at a nominal temperature $T = 294$ K (●) and $k_{n,n-1}$ values derived from equilibrium data for $\Delta G^0_{n,n-1}$ (Table 1) and eq 10 for $T = 270$ K (▲). A log base 10 scale is used for $k_{n,n-1}$ (s^{-1}) values. Note that the values due to BIRD are 4 to 6 orders of magnitude smaller.

A downward deviation of the rate constant k_{12} based on the thermochemical data (Table 1) is not indicated in Figure 5. The deviation, if present, is so small that it falls within the error limits of the equilibrium experiments. Assuming that the BIRD result leading to a lower rate for $\text{SO}_4(\text{H}_2\text{O})_{12}^{2-}$ is not due to experimental errors involving this particular hydrate, one can ask the question: Is it possible that both the BIRD result for the lower rate of the $\text{SO}_4(\text{H}_2\text{O})_{12}^{2-}$ and the rate constants based on the thermochemical data are correct. A simple analysis indicates that this is the case and that both results provide useful physical insights. It is well-known¹⁶ that, when the energy is provided by BIRD, the reactant will have a Boltzmann distribution corresponding to the temperature of the walls of the reaction chamber only when it is a very large molecule, see Figures 4 and 5 in Dunbar and McMahon^{16a} and see Williams.^{16b} This comes about because, for such molecules, the dissociation rate at the energy threshold is very low, which allows the rate of absorbed BIRD radiation to maintain a Boltzmann distribution. The $\text{SO}_4(\text{H}_2\text{O})_{12}^{2-}$ has 114 degrees of freedom and one expects it to fall between the large molecules such as proteins that maintain a Boltzmann distribution¹⁶ and the small molecules that have a highly depleted energy distribution at the threshold energy region.¹⁶ Wong and Williams¹³ expected that depletion of the energy distribution at the threshold will be present but did not specify that it might be severe.

A comparison of their reaction rates at a wall temperature of 21 °C with the expected rates at that temperature, see Figure 5, indicates that the energy depletion was quite severe. This will also be the case for the neighboring hydrates. The most stable structure of $\text{SO}_4(\text{H}_2\text{O})_{12}^{2-}$ predicted by the theoretical calculations could well have been the dominant species undergoing decomposition when the threshold is so energy depleted. This would explain the lower rate observed¹³ for the $\text{SO}_4(\text{H}_2\text{O})_{12}^{2-}$. Thus, these ions could be “magic” also in thermal dissociations but at temperatures very much lower than 21 °C, possibly as low as -100 °C, see Figure 5.

The thermal equilibrium measurements are at temperatures where the dissociation rates of the hydrates are very high and the Boltzmann distribution is maintained by rapid activation by collisions. Under these higher energy conditions, a given $\text{SO}_4(\text{H}_2\text{O})_n^{2-}$, including the $n = 12$, may partition also into isomeric structures that have somewhat higher energies. This partitioning will be driven by the lower entropy of these more disordered structures. Dissociation will then also occur from these structures and lead to a higher overall rate constant, $k_{n,n-1}$. A significantly lower $k_{12,11}$ will not be expected in this case, in

agreement with the experimental results from the thermal measurements.

4. Conclusions

(a) The entropies $\Delta S^0_{n,n-1}$ for $n = 7$ to 12 which are in the range of 21.6–17.2 cal/(deg·mol) are very low compared to $\Delta S^0_{n,n-1}$ values obtained in previous work for inner shell hydrates that are strongly bonded and tightly packed. This indicates that in the temperature range -20 to 65 °C very loose structures in the outer shell region are present where the water molecules may be able to quasitranslate over the surface of the hydrate. These experimental results are of special interest because the determination of the $\Delta S^0_{n,n-1}$ values on the basis of vibrational frequencies evaluated with ab initio calculations is expected to be unreliable when such loose structures are present.

(b) Rate constants $k_{n,n-1}$ for the dissociation reaction ($n,n-1$) can be evaluated with the present results. The $k_{n,n-1}$ values are found 3–6 orders of magnitude higher than the $k_{n,n-1}$ values determined¹³ with the BIRD technique. This large difference is attributed to the non-Boltzmann internal energy distribution expected with BIRD. The values obtained in the present work do not lead to a relatively low value for $k_{12,11}$ that would have indicated a greater stability for the $n = 12$ hydrate, as was found for the rate constants determined¹³ with BIRD. This difference can be rationalized as follows:

The dissociation $\text{SO}_4(\text{H}_2\text{O})_{12}^{2-} = \text{SO}_4(\text{H}_2\text{O})_{11}^{2-} + \text{H}_2\text{O}$ occurs at a very much lower effective excitation energy in the BIRD experiments. Under these conditions only the most stable $\text{SO}_4(\text{H}_2\text{O})_{12}^{2-}$ isomeric structure will be involved in the dissociation. At the much higher internal excitation present in the present experiments, other isomers of slightly higher energy and higher entropy will also be present as expected from the looseness of the structures discussed in (a). The dissociation of these isomers will lead to a higher $k_{12,11}$ value.

Acknowledgment. This work was supported by a Grant from the Canadian Natural Sciences and Engineering Research Council (NSERC).

References and Notes

- (1) (a) Hogg, A. M.; Haynes, R. N.; Kebarle, P. *J. Am. Chem. Soc.* **1966**, *88*, 28–31. (b) Dzidic, I.; Kebarle, P. *J. Phys. Chem.* **1970**, *77*, 1466–1474.
- (2) (a) Kebarle, P. *Annu. Rev. Phys. Chem.* **1977**, *28*, 445–476. (b) Castleman, A. W. *J. Phys. Chem. Ref. Data* **1986**, *15*, 1011. (c) Kebarle, P. *Modern Aspects of Electrochemistry*; Conway, B. E., Bockris, O. M., Eds.; Plenum Press: New York, 1974; Vol. 9, pp 1–46. (d) Lias, S. G.; Bartmess, J. E.; Liebman, J. F.; Holmes, J. L.; Levin, R.; Mallard, W. G. *J. Phys. Chem. Ref. Data* **1988**, *17*, Suppl. No. 1.
- (3) (a) Kraemer, W. P.; Dierksen, G. H. F. *Theor. Chim. Acta (Berlin)* **1972**, *27*, 265–272. (b) Kraemer, W. P.; Dierksen, G. H. F. *Chem. Phys. Lett.* **1970**, *5*, 403–465. (c) Newton, M. D.; Ehrenson, S. *J. Am. Chem. Soc.* **1971**, *93*, 4971–4990. (d) Kistenmacher, H.; Popkie, H.; Clementi, E. *J. Chem. Phys.* **1973**, *59*, 5842–5848. (e) Chandrasekhar, J.; Spellmeyer, D. C.; Jorgensen, W. L. *J. Am. Chem. Soc.* **1984**, *106*, 903–910.
- (4) Okumura, M.; Yeh, L. I.; Lee, Y. T. *J. Phys. Chem.* **1988**, *88*, 79–91.
- (5) Yamashita, M.; Fenn, J. B. *J. Phys. Chem.* **1984**, *88*, 4451–4459.
- (6) Blades, A. T.; Jayaweera, P.; Ikononou, M. G.; Kebarle, P. *J. Chem. Phys.* **1990**, *92*, 5900–5906.
- (7) Blades, A. T.; Kebarle, P. *J. Am. Chem. Soc.* **1994**, *116*, 10761–10766.
- (8) Boldyrev, A. I.; Simons, J. *J. Phys. Chem.* **1994**, *88*, 2298–2300.
- (9) Blades, A. T.; Klassen, J. S.; Kebarle, P. *J. Am. Chem. Soc.* **1995**, *117*, 10563–10571.

- (10) Blades, A. T.; Klassen, J. S.; Kebarle, P. *J. Am. Chem. Soc.* **1996**, *118*, 12437–12442.
- (11) Peschke, M.; Blades, A. T.; Kebarle, P. *J. Am. Chem. Soc.* **2002**, *124*, 11519–11530.
- (12) Wang, X. B.; Nicholas, J. B.; Wang, L. S. *J. Chem. Phys.* **2000**, *113*, 10837–10840.
- (13) Wong, R. I.; Williams, E. R. *J. Phys. Chem. A* **2003**, *107*, 10976–10983.
- (14) (a) Peschke, M.; Blades, A. T.; Kebarle, P. *J. Phys. Chem. A* **1999**, *102*, 9978–9985. (b) Peschke, M.; Blades, A. T.; Kebarle, P. *J. Am. Chem. Soc.* **2000**, *122*, 10440–10449.

- (15) (a) Su, T.; Bowers, M. T. *J. Chem. Phys.* **1973**, *58*, 3027 (b) Su, T.; Bowers, M. T. *Int. J. Mass Spectrom. Ion Phys.* **1975**, *17*, 211–212.
- (16) (a) Dunbar, R. C.; McMahon, T. B. *Science* **1998**, *279*, 194–197. (b) Price, W. D.; Williams, E. R. *J. Phys. Chem. A* **1997**, 8844–8852.
- (17) The residence time of ions in the reaction chamber is in the 200 μs range.¹¹ For the hydration equilibria to establish rapidly in the reaction chamber, the half-life of the forward and reverse reactions must be much shorter than the residence time of the ions in the reaction chamber. Furthermore, the pressure of the bath gas N_2 (10 Torr) may be too low to lead to dissociation and association rates at the high-pressure limit. This suggests that the $k_{n,n-1}$ values at the high-pressure limit must be in the 10^5 – 10^6 s^{-1} , range.